

Reference:

Lequesne, R. D., Parra-Montesinos, G. J. and Wight, J. K. (2009), "Test of a Coupled Wall with High Performance Fiber Reinforced Concrete Coupling Beams," *Thomas T. C. Hsu Symposium: Shear and Torsion of Concrete Structures*, SP-265, American Concrete Institute, Farmington Hills, MI.

# Test of a Coupled Wall with High Performance Fiber Reinforced Concrete Coupling Beams

by Rémy Lequesne, Gustavo Parra-Montesinos, and James K. Wight

Synopsis:

Results from the test of a large-scale coupled-wall specimen consisting of two T-shaped reinforced concrete structural walls joined at four levels by precast coupling beams are presented. Each coupling beam had a span length-to-depth ratio ( $\ell_n/h$ ) of 1.7, and was designed to carry a shear stress of  $7\sqrt{f'_c}$ , [psi] ( $0.59\sqrt{f'_c}$ , [MPa]). One reinforced concrete coupling beam was included along with three strain-hardening, High-Performance Fiber Reinforced Concrete (HPFRC) coupling beams to allow a comparison of their behavior. When subjected to reversing lateral displacements, the system behaved in a highly ductile manner characterized by excellent strength retention to drifts of 3% without appreciable pinching of the lateral load vs. drift hysteresis loops. The reinforced concrete structural walls showed an excellent damage tolerance in response to peak average base shear stresses of  $4.4\sqrt{f'_c}$ , [psi] ( $0.34\sqrt{f'_c}$ , [MPa]). This paper presents the observed damage patterns in the coupling beams and the structural walls. The restraining effect provided by the structural walls to damage-induced lengthening of the coupling beams is discussed and compared to that observed in component tests. Finally, the end rotations measured in the coupling beams relative to the drift of the coupled-wall system are also presented.

Keywords: coupling beam, coupled wall, high performance fiber reinforced concrete (HPFRC), precast, seismic, shear

Rémy Lequesne, ACI member, is a PhD student in Civil Engineering at the University of Michigan, Ann Arbor. He was the 2007-2008 ACI Pankow Foundation Fellowship recipient, and is an Associate Member of ACI Committee 374, Performance-Based Seismic Design of Concrete Buildings. His research interests include the behavior and design of reinforced concrete members, the mechanical and structural behavior of high-performance fiber-reinforced concrete, and the earthquake resistant design of reinforced concrete structures.

Gustavo J. Parra-Montesinos, ACI member, is an Associate Professor of Civil Engineering at the University of Michigan, Ann Arbor. He is Secretary of ACI Committee 335, Composite and Hybrid Structures; and a member of ACI Committee 318, Structural Building Code, and Joint ACI-ASCE Committee 352, Joints and Connections in Monolithic Concrete Structures. His research interests include the behavior and design of reinforced concrete, hybrid steel-concrete, and fiber reinforced concrete structures.

James K. Wight, FACI, is a Professor of Civil Engineering at the University of Michigan, Ann Arbor. He is Past Chair of ACI Committee 318, Structural Concrete Building Code and ACI Committee 318-E, Shear and Torsion, and is a member of Joint ACI-ASCE Committees 352, Joints and Connections in Monolithic Concrete Structures, and 445, Shear and Torsion. His research interests include the earthquake-resistant design of reinforced concrete structures and the use of high-performance fiber-reinforced concrete in critical regions of such structures.

## INTRODUCTION

Concrete structural walls are commonly used as the primary lateral force resisting system for both medium- and high-rise concrete and steel frame structures. Due to their stiffness and strength, structural walls attract a considerable amount of lateral force when subjected to earthquake induced displacement reversals. The efficiency of a structural wall system can be improved by proper coupling of two or more consecutive walls through the use of short coupling beams. This coupling action reduces the demand for flexural stiffness and strength from the individual walls by taking advantage of their axial stiffness, strength, and the distance between the centroidal axes of adjacent walls to provide additional resistance to overturning moment.

For satisfactory performance of a coupled-wall system during a seismic event, the short coupling beams must retain a significant, and predictable, strength and stiffness through large displacement reversals. To ensure adequate coupling beam ductility is achieved, the ACI Building Code (ACI Committee 318, 2008) requires that diagonal reinforcement be provided to resist all of the shear demand in short and highly stressed coupling beams. This reinforcement detail has been shown by many researchers to provide a stable behavior under earthquake-type displacement reversals, but can be difficult and time consuming to construct. Recent coupling beam component tests (Canbolat, Parra-Montesinos, and Wight, 2005; Lequesne et al., 2009) have demonstrated that precasting coupling beams with strain-hardening, High Performance Fiber Reinforced Concrete (HPFRC) can simplify the construction process without sacrificing performance. The HPFRC coupling beams have exhibited a highly ductile behavior when subjected to large displacement reversals, despite requiring significantly simpler reinforcement detailing than comparable reinforced concrete beams.

The impact that the ductility exhibited by HPFRC coupling beams at the component level has on a coupled-wall system, however, has not been studied experimentally. The test described herein seeks to study the interaction between precast HPFRC coupling beams and structural walls, with special attention being paid to the ductility and strength retention of the system and the deformation demands that each system component is subjected to.

In addition to the performance of the system, the construction process required for this specimen is considered to be of great importance. The most significant limitation of the current design approach is the cumbersome reinforcement that is time consuming and difficult to assemble on-site. For the specimen described herein, the precast coupling beams were inserted between the wall's longitudinal reinforcing bars, and supported by wall formwork. The remaining wall reinforcement was subsequently placed without significant interference from beam reinforcement, which protruded horizontally from the ends of the precast member and through the wall boundary element, as shown in Fig. 1. The construction of this specimen demonstrated that HPFRC coupling beams can be precast and easily embedded into cast-in-place structural walls with minimal reinforcement interference.

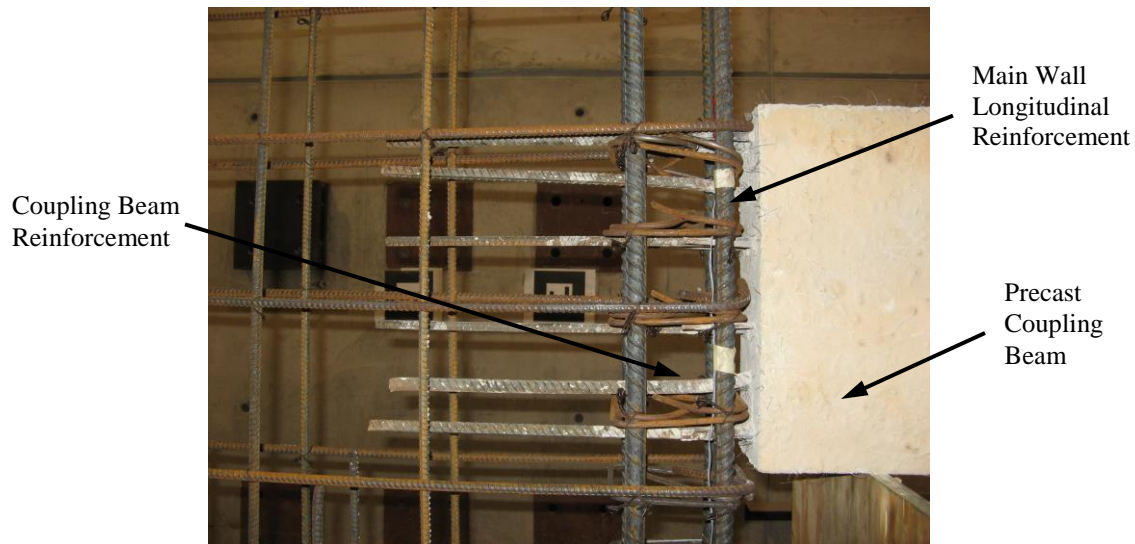


Fig. 1 – Precast coupling beam embedment detail

### RESEARCH SIGNIFICANCE

An experimental investigation of the implications of using precast HPFRC coupling beams on the design, constructability, and performance of coupled walls is presented. More specifically, this project seeks to: 1) demonstrate the ease with which precast coupling beams can be embedded in cast-in-place structural wall systems, 2) provide a comparison between various coupling beam details when subjected to similar deformation demands, and 3) study the interaction between HPFRC coupling beams, slabs, and structural walls.

### GENERAL DESIGN AND TEST SETUP

A diagram of the coupled-wall specimen is shown in Fig. 2. Each of the coupling beams had a slightly different reinforcement layout, shown in Fig. 3, which allowed for a comparison of various reinforcement layouts. Slabs were built at the second and fourth levels to facilitate lateral load application. Slab reinforcement placed perpendicular to the loading direction was continuous through the structural walls, but not the precast coupling beams. The slabs provided an opportunity to observe the interaction between the precast coupling beams and the adjacent slab, and to evaluate the need for design modifications to minimize damage at this connection.

For design of the specimen, the base of each wall was assumed to be fixed, which was achieved experimentally through the use of deep reinforced concrete foundation elements bolted directly to the laboratory strong floor. A vertical force, equivalent to an axial stress of 7% of the design  $f'_c$ , based on the gross area of the walls, was applied at the second story through external prestressing tendons anchored at the bottom of the foundation elements. Steel tube sections cast through each wall above the second story slab transferred the force from the external tendons into the walls. Hydraulic jacks were used to apply this vertical force before any lateral displacement was applied, and held it constant throughout the duration of the test. This level of gravity load is consistent with current design practice for structural walls and was sufficient to offset a majority of the uplift force resulting from the coupling of the walls.

The test setup, shown in Fig. 4, was used to pseudo-statically apply lateral displacement (and load) through the slabs cast at the second and fourth levels. The actuator mounted on the fourth level applied a predetermined sequence of reversing lateral displacements, while the actuator at the second level applied a force equivalent to 60% of the force applied by the top actuator. These lateral forces were transferred to the coupled walls through a yolk and four channel sections that were attached to the top and bottom of the outer edges of the slabs. This was intended to allow for a distribution of lateral force to each of the structural walls that is similar to the load transfer mechanism that develops in a normal building system.

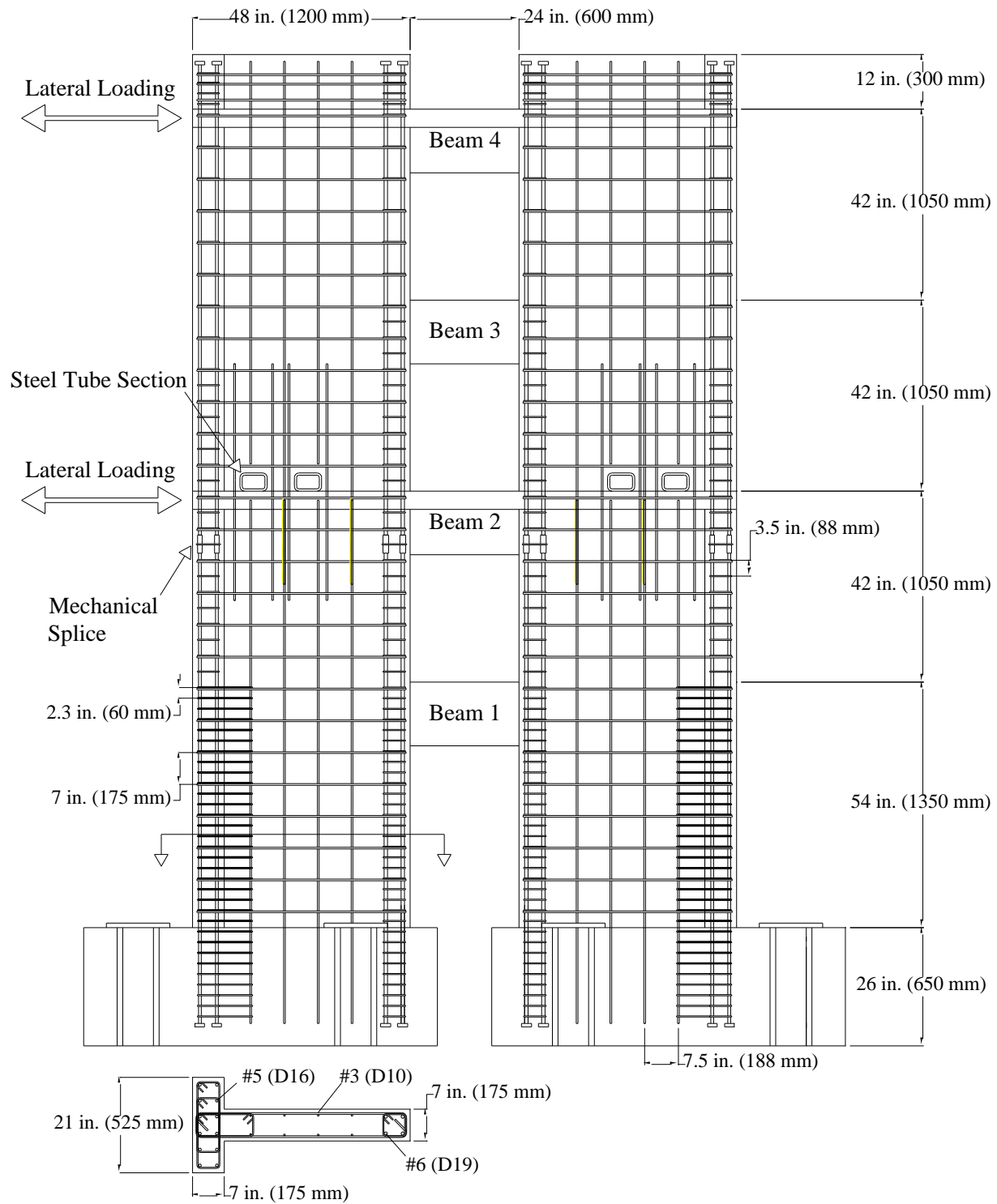
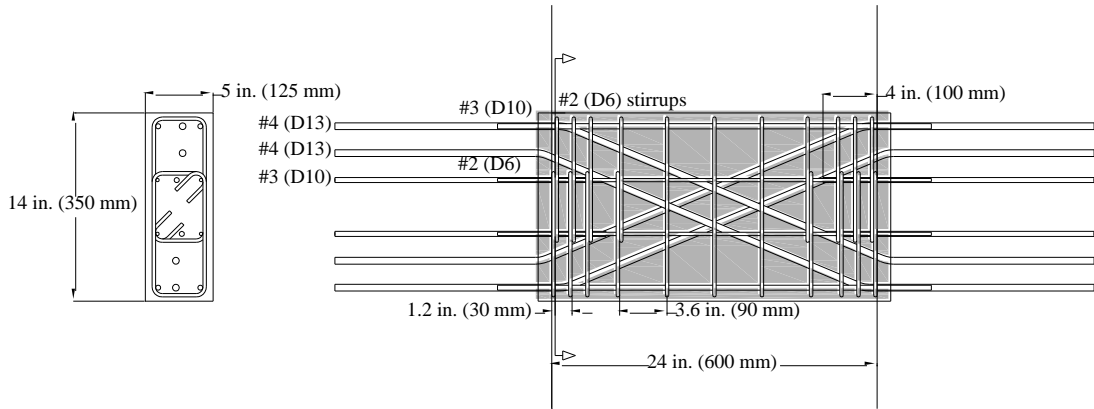
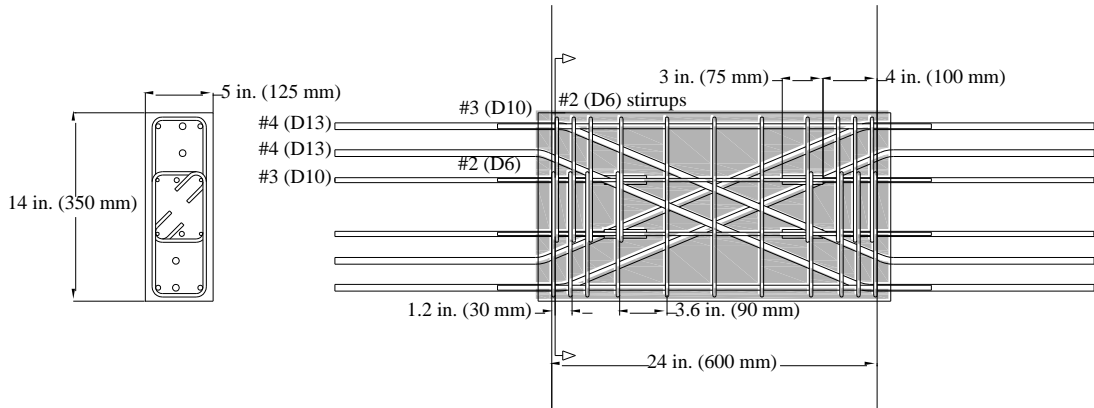


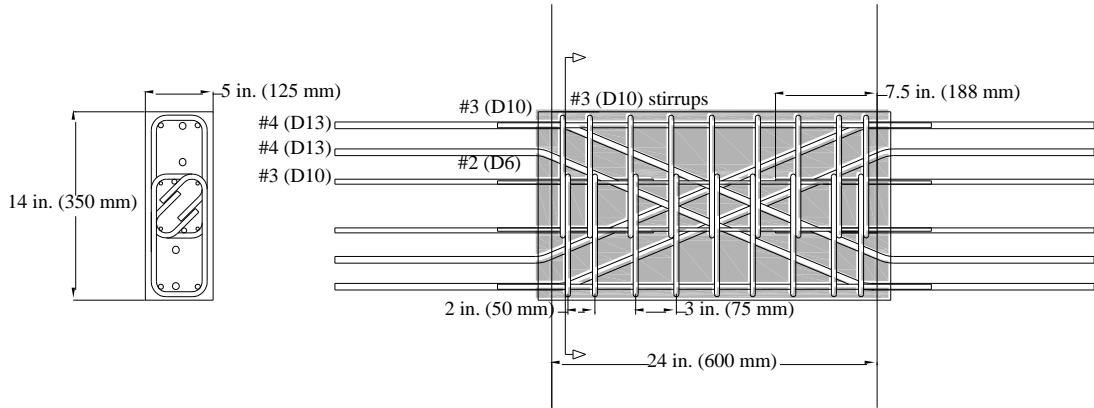
Fig. 2 - Coupled-wall specimen reinforcement



(a) Beam 1, 4: Bonded FRC



(b) Beam 3: Debonded FRC



(c) Beam 2: RC

Fig. 3 - Coupling beam reinforcement

Efforts were made throughout the construction of the specimen to be as realistic as possible in terms of both construction methods and sequencing. It was felt that this approach was critical for gauging the possible construction scheduling advantages gained by incorporating precast coupling beams. The construction process consisted of first precasting the coupling beams and storing them, ready for placement. The construction of each wall story began with tying the wall reinforcement into position and then placing enough of the wall formwork to support the precast beam. The beam was then slid into position with an overhead crane and placed on the formwork that supported it fully until the wall concrete was placed. Overlapping U-shaped stirrups were used to provide confinement to the wall boundary element in the region where the coupling beam reinforcement intersected the longitudinal wall reinforcement, as shown in Fig. 1. Ensuring adequate anchorage for the special transverse reinforcement is critical, yet the preferred detail is dependent on the layout of the wall boundary element. The detail selected for this specimen consisted of overlapping U-shaped stirrups anchored by 135-degree bends around the longitudinal reinforcement. Finally, the wall formwork assembly was completed and the concrete was placed. The formwork was then removed, moved up the wall, and the sequence described above was repeated. The process proved to be efficient.

At the second and fourth levels, where a slab was also present, the top of the precast coupling beam was placed to be flush with the top of the slab. Although the slab concrete was cast against the precast beam, no reinforcement crossed this cold joint. It has been demonstrated that the influence of a slab on the cyclic response of coupling beams is limited to minor stiffening in early drift cycles (Paulay and Taylor, 1981; Gong and Shahrooz, 2001). This is due to the much lower stiffness observed in slabs relative to coupling beams when subjected to reversed cyclic loads. After the influence of the slab degrades, the slab-beam is expected to behave very similarly to a beam component without a slab. Therefore, no attempt was made to encourage interaction between the slab and precast coupling beam, which simplified casting and placement of the precast coupling beam without sacrificing performance.



Fig. 4 – Photo of test setup and specimen

## INSTRUMENTATION

To record the performance of the coupled-wall specimen, strain gauges, linear potentiometers, inclinometers, load cells, and optical position sensors were used. Strain gauges were placed on coupling beam reinforcement, wall longitudinal reinforcement at every level, and transverse reinforcement within the first story of the wall. Linear potentiometers measured deformations in the second, third and fourth coupling beams, monitored

the lateral displacement at the second and fourth levels, and measured vertical deformations along the edges of both structural walls. Inclinometers were used to monitor wall rotations at the second, third, and fourth levels. Load cells measured the forces applied laterally to the specimen, and the vertical force applied at the second level was monitored by hydraulic pressure gauges. Finally, an optical system (Optotrak Certus from Northern Digital Inc.) was used to track the location of 144 independent markers placed in a grid covering the first story of both walls and the first coupling beam. This optical system provided reliable data that were used to calculate deformations, rotations, and displacements.

## MATERIAL PROPERTIES

Recent work at the University of Michigan (Liao et al., 2006) has led to the development of a flowable HPFRC with a 1.5% volume fraction of high-strength hooked steel fibers. The mixture also includes coarse aggregate with a maximum nominal size of 0.5 in. (13 mm). The properties of the fibers, as specified by the manufacturer, are summarized in Table 1. This mixture was selected for the precast HPFRC coupling beams used in this study.

Results from compressive tests of 4 in. by 8 in. (100 mm by 200 mm) cylinders performed at 28 days and near the test dates are shown in Table 2. The test day values of  $f'_c$  are used throughout this paper. A representative compressive constitutive response, based on cylinder tests, is shown in Fig. 5, and was used for design purposes. A parabola was assumed to represent the ascending branch, followed by a shallow linear descending branch that accounted for the confinement provided by the distributed fiber reinforcement. A maximum useable concrete compressive strain of 0.8% was assumed.

Length (in./mm)		Diameter (in./mm)		L/d	Minimum Tensile Strength (ksi/MPa)	
1.2	30	0.015	0.38	80	330	2300

Table 1 – Hooked steel fiber properties

Portion of Specimen	Fibers?	28-Day Tests								Test Day $f'_c$ (ksi/MPa)	
		$f'_c$ (ksi/MPa)		ASTM 1609 Flexural Tests							
				$\sigma_{fc}^a$ (psi/MPa)		$\sigma_{peak}^b$ (psi/MPa)		$\sigma_{(\delta=L/150)}^c$ (psi/MPa)			
CB-1	Y	5.5	38	765	5.3	1090	7.5	540	3.7	10.4	72
CB-2	N	5.3	37							9.8	68
CB-3	Y	5.5	38	765	5.3	1090	7.5	540	3.7	10.4	72
CB-4	Y	6.0	41	850	5.9	1120	7.7	610	4.2	10.8	74
Foundation	N	5.0	34							7.8	54
Wall 1 <sup>st</sup> lift	N	5.3	37							7.0	48
Wall 2 <sup>nd</sup> lift	N	4.1	28							6.7	46
Wall 3 <sup>rd</sup> lift	N	5.5	38							6.6	45
Wall 4 <sup>th</sup> lift	N	6.9	48							9.5	65

<sup>a</sup> Bending stress at first crack,

<sup>b</sup> Bending stress at peak stress,

<sup>c</sup> Bending stress at a deflection of L/150

Table 2 – Concrete properties

Portion of Specimen	Bar Size	Yield Stress (ksi/MPa)		Ultimate Stress (ksi/MPa)	
Coupling Beams	#3 (D10)	79.4	550	121	830
	#4 (D13)	76.9	530	115	790
Structural Wall	#3 (D10)	74.2	510	112	770
	#5 (D16)	67.2	460	109	750
	#6 (D19)	68.0	470	109	750

Table 3 – Steel reinforcement properties

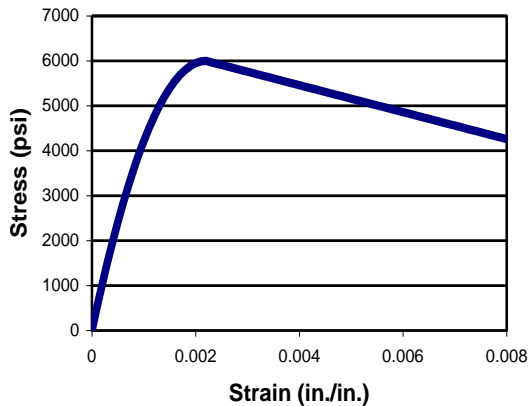


Fig. 5 – Compression constitutive model

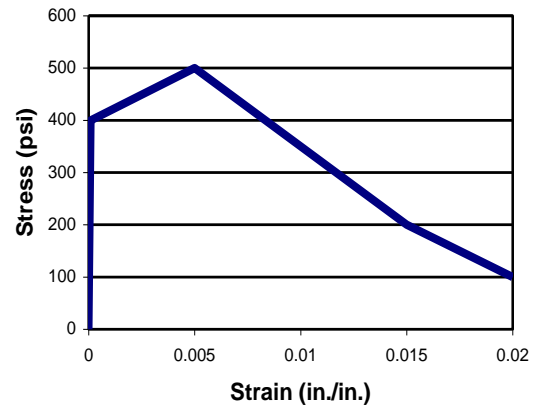


Fig. 6 – Tension constitutive model

Average tensile properties previously determined for this HPFRC mixture (Liao et al., 2006) were used for design of the test specimens. The representative tensile stress-strain response, shown in Fig. 6, has a peak tensile stress of 500 psi (3.4 MPa) at 0.5% strain, 25% higher than the first cracking stress. This peak is followed by a gradual decrease in tensile stress capacity. On average, tensile specimens still carried 50% of their peak tensile stress at 1.4% strain.

Bending tests were also performed on short beams with dimensions of 6 in. by 6 in. by 20 in. (150 mm by 150 mm by 500 mm), in accordance with ASTM C1609–05. These tests were performed 28 days after casting each HPFRC coupling beam to characterize the bending properties of the HPFRC used in this study. The results of these tests are summarized above in Table 2 by the following three values: the equivalent bending stress at first crack ( $\sigma_{fc}$ ), peak stress ( $\sigma_{peak}$ ), and at a deflection of  $L/150$ , where  $L$  is the beam span length of 18 in. (450 mm). All tests showed pronounced deflection hardening behavior, with peak bending stresses occurring near deflections of  $L/800$  which exceeded the first cracking stress by more than 30%.

The tensile stress-strain properties of the reinforcing steel used for the construction of this specimen were evaluated by direct tensile tests on representative coupons. The measured yield and ultimate stresses from these tests are summarized in Table 3.

## SPECIMEN DESIGN

### Coupling Beam Design

Three different reinforcement details, shown in Fig. 3, were selected for the coupling beams in this system. Care was taken to ensure that all of the designs exhibited similar initial stiffnesses and calculated ultimate flexural capacities, which resulted in shear stresses near  $7\sqrt{f'_c}$ , [psi] ( $0.55\sqrt{f'_c}$ , [MPa]). This was done to prevent any particular beam from attracting more shear than the others. One unavoidable design issue is the contribution of the



fiber reinforcement to the moment capacity of fiber reinforced coupling beams, compared to conventional reinforced concrete beams. Although this contribution will increase the beam capacity near and at the first yield point, the impact will diminish at larger deformations. Significant yielding was observed in the diagonal reinforcement of all four coupling beams by the time the system drift, defined as the lateral displacement of the top slab divided by the wall height off of the foundation, reached 1%. Thus, it is reasonable to assume that shears were relatively evenly distributed between the beams at these larger drifts.

The first coupling beam design, which was used as Beams 1 and 4 in the coupled wall, is labeled “Bonded FRC” and is shown in Fig. 3(a). This design is comparable to the component tests reported by Lequesne et al. (2009). The following notes should be made on this design:

- Diagonal bars were provided to carry approximately half of the expected ultimate shear capacity and to improve the rotational ductility at the beam ends, where plastic hinges were expected to develop. The diagonal bar contribution to shear was originally targeted to be close to 40% of ultimate, but due to scaling issues, a slightly larger diagonal bar contribution resulted. No special transverse reinforcement, except for the beam ends, was provided to prevent buckling of the diagonal bars because strain-hardening HPFRC composites have been shown to confine diagonal reinforcement and arrest any tendency to buckle (Canbolat, Parra-Montesinos, and Wight, 2005).
- Longitudinal reinforcement was provided, but only embedded 3 in. (75 mm) into the walls. This is commonly done to limit the contribution of the longitudinal reinforcement to the flexural capacity of the coupling beam.
- To strengthen the interface between the precast fiber reinforced beam and the structural wall, and to encourage plastic hinging to develop inside the fiber reinforced section, dowel bars were provided across the beam-wall interface and terminated 4 in. (100 mm) into the beam. The high bond stress developed between fiber reinforced concrete and reinforcing bars, addressed by Chao (2005), made this very short development length sufficient to yield the dowel bars near the interface.
- Transverse reinforcement was provided in the beam for the first  $h/2$  away from the wall face to confine the beam plastic hinge regions. Stirrups were provided throughout the remaining span to carry approximately one-half of the expected shear.

The second coupling beam design, which was used as Beam 3 in the coupled wall, is labeled “Debonded FRC” and is shown in Fig. 3(b). This design was identical to the previous design, with one detailing change. Within the beam, the dowel bars were extended 3 in. (75 mm) beyond the 4 in. (100 mm) development length and debonded over that added length. The term “debonding” is used here to describe the use of mechanical means to prevent the fiber reinforced concrete from bonding with the reinforcing bar. This was accomplished by wrapping the bar with a few layers of plastic sheeting, and sealing it with tape. The intent was to delay the development of a single failure plane by eliminating the disturbance resulting from the physical discontinuity of the terminated bar. The motivation for this detail came from the observation that the dowel bars in previous component tests were successful in moving the ultimate failure plane away from the interface to the plane where the dowel bars were terminated. If possible, it would be advantageous to spread that flexural yielding out through a larger portion of the coupling beam, thus further delaying the localization of rotations.

The third coupling beam design, which was used as Beam 2 in the coupled wall, is labeled “RC” and is shown in Fig. 3(c). This reinforced concrete beam design was unique because it investigated the potential for precasting non-fiber reinforced concrete coupling beams, which could offer construction time-savings if proven to be successful. To account for the precasting and embedment of this coupling beam, the ACI Building Code requirements were modified, and a detail more similar to the “Bonded FRC” design discussed above was selected. The following modifications to the “Bonded FRC” design were made to account for the lack of fiber reinforcement.

- The dowel bars were extended 7.5 in. (188 mm) into the span of the beam. This longer development was required to compensate for the lower bond stress capacity developed between conventional concrete and reinforcing steel, compared to fiber reinforced concrete.
- The transverse reinforcement provided in the plastic hinge region was approximately doubled (larger diameter) to compensate for the loss of confinement from the fiber reinforcement.
- The transverse reinforcement in the remaining span was approximately doubled (larger diameter and reduced spacing) when compared to the fiber reinforced beams. This provided confinement to the diagonal bars, preventing buckling, and also compensated for the loss of the contribution of the fiber reinforcement to the shear capacity of the section.

## Structural Wall Design

The coupling beam dimensions and detailing were of special interest in this project, and thus, they were the initial focus of the coupled wall design. The structural walls were subsequently designed following the ACI Building Code to provide the required overturning moment capacity and ductility for the coupled-wall system to behave realistically.

The wall shear design was based on the expected ultimate capacity of the system, assuming that a mechanism controlled by flexural hinging in the base of both walls and in each of the beams would develop. To resist the expected shear demand, the wall concrete was assumed to carry a shear stress equivalent to  $2\sqrt{f'_c}$ , [psi] ( $0.17\sqrt{f'_c}$ , [MPa]) and wall transverse reinforcement, anchored by alternating 90- and 135-degree bends and representing a transverse reinforcement ratio of 0.45%, was provided to resist the remaining shear.

The coupling ratio, which expresses the overturning moment resistance from the wall axial forces generated by the “coupling action” as a fraction of the total overturning moment resistance of the coupled-wall system, was selected to be between 0.35 and 0.40. While some researchers have used alternative definitions for the coupling ratio, it is defined here based on the calculated ultimate flexural capacities of the system components. This is a more reasonable definition for this system, because the ductile response expected from fiber reinforced coupling beams increases the likelihood that a plastic mechanism will develop in which all beams and walls are concurrently near their respective ultimate capacities. Testing of the system demonstrated that a coupling ratio of approximately 0.4 was attained at a system drift near 0.75%, and sustained out to drifts past 2.5%. Given this result, defining the coupling ratio using ultimate capacities appears to be reasonable for systems similar to the one tested and coupled with HPFRC coupling beams. The axial effects in each structural wall due to the combined shearing of the coupling beams and the externally imposed gravity load are critical for the flexural capacity predictions at the base of each wall, and were thus accounted for in the design of the system.

T-shaped wall sections were used to simulate the fact that most coupled walls in a core-wall structural system have a flange at the end of the wall away from the coupling beam. Thus, such walls tend to have different flexural capacities when subjected to “positive” or “negative” bending about their principal axis, as was the case for the walls used in this test structure. These flanged sections had the added benefit of providing improved lateral stability during testing.

ACI Building Code compliant mechanical couplers were used at mid-height of the walls to splice longitudinal reinforcement in the boundary elements. Mechanical anchorages were used to develop that same reinforcement in the foundation block and in the short extension at the top of the walls. Conventional lap splices were used for the distributed wall web reinforcement.

## **RESULTS**

### Overall Behavior and Damage

A plot of the overturning moment vs. drift response of the coupled-wall specimen is shown in Fig. 7, along with the predicted capacity with and without the effect of the coupling beams. Assuming the plastic mechanism described above developed, and accounting for the measured concrete and reinforcing steel properties, the system overturning moment capacity was under-predicted by only approximately 5%. Ninety percent of the system’s ultimate overturning moment capacity was maintained up to drifts of 3%, which is a significant level of deformation for coupled reinforced concrete shear walls. When the system drift exceeded 2.5%, the coupling beams were all subjected to drift demands exceeding 4.5%. Coupling beam drift is used herein to describe the chord rotation referenced in ASCE/SEI 41 (2007). The observed coupling beam drift demands exceeding 4.5% emphasize the need for highly ductile coupling beams, and the stable system response is evidence that the coupling beams used in this system were capable of withstanding these drift demands. Furthermore, the full hysteresis loops show no appreciable pinching, which indicates that the response of the system was governed by flexural hinging in the bases of the walls and at the ends of the coupling beams, as predicted.

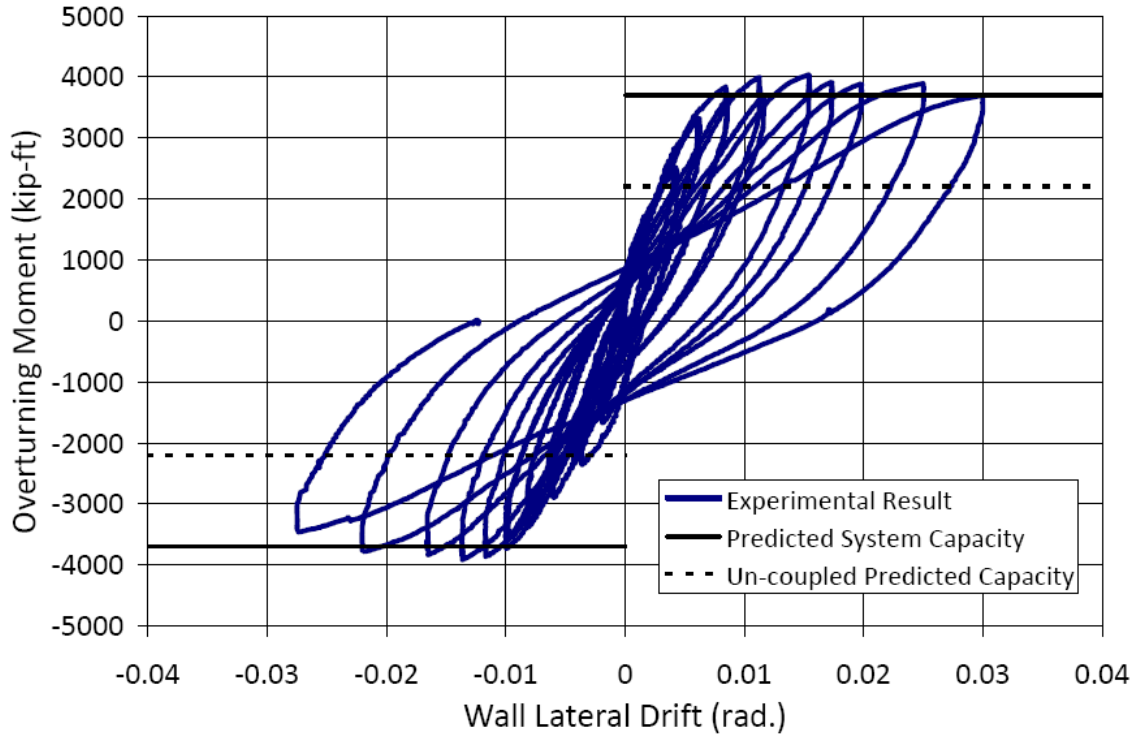


Fig. 7 - Overturning moment vs. wall lateral drift response

Throughout the testing process, a coordinated team of students carefully monitored development of cracks over the full height of the specimen. At a system drift of 0.25%, diagonal-shear cracks were observed in the first story of the “compression” wall. Throughout this paper, “compression” wall is used to refer to the wall that, due to the coupling action of the beams, was subjected to increased compression within a particular loading half-cycle. As previously shown (Aktan and Bertero, 1984; Teshigawara et al., 1998b), this increased compression caused the compression wall to attract a higher shear stress than the opposing “tension” wall, resulting in more pronounced shear cracking on the compression side of the system. Similar diagonal-shear cracking developed in the first story of the opposing wall after reversal of the loading direction.

At a system drift of 0.5%, diagonal-shear cracking was observed in all four coupling beams. Also at this drift level, the following pattern of damage was first observed in the lower levels of the coupled wall. Diagonal cracks formed in the second story of the tension wall, progressed through the coupling beam between the first and second stories, and extended as diagonal cracks through the first story of the compression wall to the foundation. This crack pattern indicated that at low drifts, the coupling of the system was sufficiently high to cause the walls to act as one unit with a prominent diagonal compression strut extending through the first two levels of the wall. Although diagonal-shear cracking was prominent in both walls during early drift cycles, the transverse reinforcement ( $\rho_t = 0.45\%$ ) successfully arrested the opening of these diagonal cracks. This allowed a ductile flexural mechanism to develop and accommodate the rotation demands placed on the walls.

The ACI Building Code requirements for structural wall design provided adequate shear resistance and confinement of longitudinal reinforcement to allow for a stable flexural mechanism to develop in the base of both walls. Once the walls and coupling beams reached their respective flexural capacities, which occurred near a system drift of 0.75%, very little additional diagonal cracking was observed in the structural walls. Further increases in lateral drift caused a wider opening of flexural cracks in the walls, and progressively more severe damage to occur in the coupling beams. The test was terminated once the integrity of the structure had been compromised by the fracturing of diagonal reinforcement in the coupling beams and flexural reinforcement in the walls.

Due to the termination of coupling beam flexural reinforcement only 3 in. (75 mm) into the wall, the moment capacity near the beam-wall interface was lower than within the beam span. The bars were terminated to be consistent with current design practice in the United States, but due to the modified flexural and shear design of these coupling beams, the flexural reinforcement represented a higher reinforcement ratio than would commonly be used in practice. The resulting plane of weakness where the coupling beam moment demands are greatest led to a localization of rotations at the precast beam/wall interface. The result was crushing and spalling of the wall concrete near the interface at system drifts exceeding 2.5%, which preceded the development of a more desirable damage pattern within the precast beam. Any meaningful comparison of the respective coupling beam reinforcement layouts was thus impossible. This undesirable pattern of damage at the interface between the precast section and the wall was not observed in component tests (Lequesne et al., 2009), where the flexural reinforcement was fully developed into the wall. Despite this undesirable localization of damage, the coupling ratio and ductility of the overall system were not compromised. In a second coupled-wall specimen, currently being tested, this reinforcement is fully developed into the wall, which will likely force damage to localize within the span of the coupling beam, as observed in component tests. This will allow for a more direct comparison of the beam designs that was not possible in this test.

The first yielding in the system was observed in the diagonal reinforcement of all four coupling beams, and was followed by yielding along the tension face of the compression wall. The T-shaped wall section provided a wider compression zone in the compression wall, resulting in a smaller depth to the neutral axis and thus, larger tensile steel strains and rotations despite the significantly higher axial loads acting on the compression side of the system. This trend continued throughout the test, with larger rotations consistently being observed in the base of the wall on the compression side of the system relative to the tension side.

The interaction between the slab and the precast coupling beam was also carefully observed throughout the test. Because no reinforcement was provided across the interface between the precast section and the adjacent slab, the potential for relative vertical displacements requiring repair was a concern. Minor cracking along the slab-beam interface was first observed at a system drift of 1.5%. Measurable relative vertical displacements of approximately 0.125 in. (3 mm) were observed between the top of the precast section and the top of the slab at system drifts exceeding 2.5%, indicating a de-coupling of their respective responses.

### Elongation of Coupling Beams

When reinforced concrete members are subjected to cyclic displacements large enough to cause significant cracking and yielding of the reinforcement, it is widely acknowledged that the cracks will not close completely upon reversal of the loading direction. Thus, reinforced concrete members have a tendency to expand longitudinally when subjected to earthquake-type cyclic displacements. In most design cases, the resulting axial strain is either too small or insufficiently restrained to cause significant axial forces to develop. However, the large drift demands placed on short coupling beams result in a strong tendency to expand longitudinally, and the adjacent structural walls and surrounding slab should provide non-negligible resistance to this expansion, as identified by Teshigawara et al. (1998a).

In component tests, few researchers have addressed longitudinal expansion of coupling beams and the possible axial forces that may develop as a result. Most experimental work has allowed for unlimited axial movement, which has been reported to be as high as 4.0% (Kwan and Zhao, 2002; Zhao and Kwan, 2003). In recent tests of coupling beam components with aspect ratios ( $\ell_n/h$ ) of 1.75 (Lequesne et al., 2009), longitudinal expansion was partially restrained, which led to maximum average axial strains between 0.5-1.0%. The result was the development of axial forces within the coupling beams as high as 55% of the applied transverse shear force at coupling beam drifts over 4%.

The coupled-wall test described herein provided an opportunity to observe the magnitude of longitudinal beam strains permitted by a realistic coupled-wall system. Fig. 8 shows the measured average axial strains of the coupling beams at all four levels plotted against the drift imposed at the top of the system. The negative axial strain (compression) observed in the coupling beam at the first level is evidence of a significant axial force acting on this member throughout the test. This axial force resulted in a shifting of base shear towards the compression side of the system consistent with previously tested coupled wall systems (Aktan and Bertero, 1984; Teshigawara et al., 1998b). This may support the observation, based on wall crack patterns, that a diagonal compression strut developed through

the first two stories of the system. While the development of this strut may partially have been an artifact of the loading mechanism, the large axial force developed in the first coupling beam warrants further investigation given the strong influence it may have on the response of coupling beams.

Positive (tension) axial strains were observed in the other three beams, with a general trend towards larger axial strains further from the foundation. The coupling beam at the second level did expand longitudinally, with measured maximum axial strains on the order of 0.75%. If correlated with the component tests cited previously, axial strains of this magnitude indicate significant restraint from the adjacent walls, and thus, the development of a significant axial compression force that will affect the capacity and ductility of the coupling beam. The coupling beam expansions at the third and fourth levels were somewhat larger than at the lower levels; however, the beam at the third level exhibited the largest axial strains. This result can be explained by the presence of the slab around the beam at the fourth level, which is evidence that a slab adjacent to a coupling beam may appreciably affect the axial restraint of the beam. This restraint appears to be large enough to develop axial forces in the coupling beam, regardless of the diminished restraint provided by the walls at a point further from the foundation. The extent to which these observations apply to taller and monolithically cast coupled-wall systems will need to be investigated further.

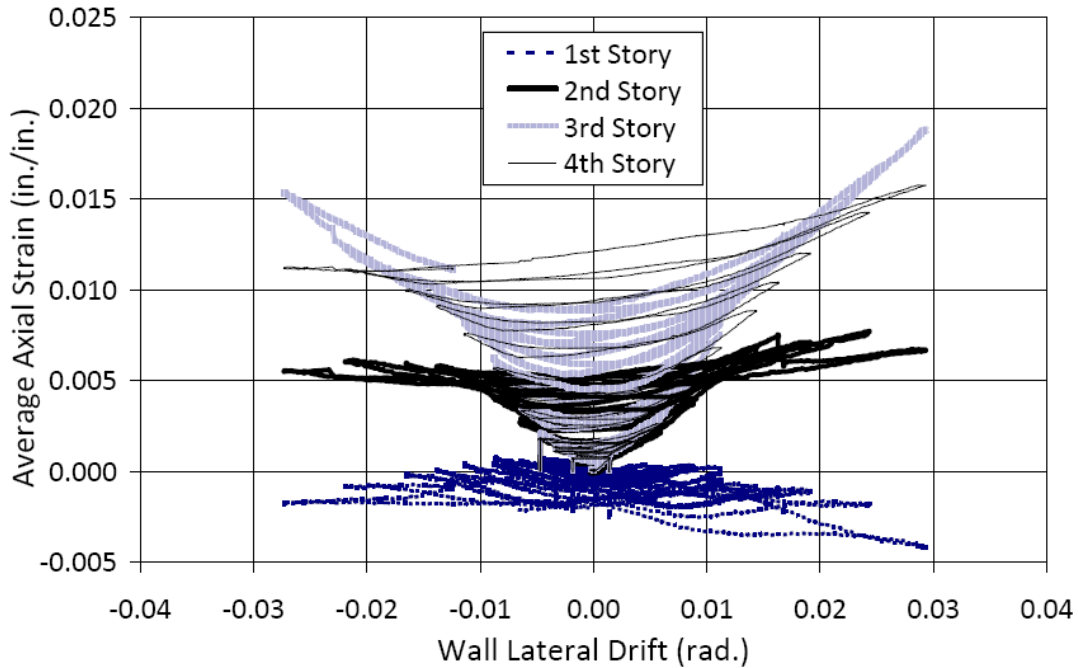


Fig. 8 - Coupling beam longitudinal strains

#### Beam/Wall Rotations

More often than not, the design of coupled-wall structural systems is motivated by a need to control the lateral drift of a structure. The design level drifts assumed for coupling beams within the coupled system are then estimated relative to the expected system drift as a function of the distance between the centroidal axes of the structural walls. This relationship is represented by:

$$\theta_b = \frac{\theta_w \cdot \ell}{\ell_b + h_b} \quad (1)$$

where  $\theta_b$  = coupling beam rotation,  $\theta_w$  = wall rotation,  $\ell$  = distance between the centroidal axes of the walls,  $\ell_b$  = clear span of coupling beam, and  $h_b$  = height of coupling beam.

The  $h_b$  term in the denominator provides an estimate of the length over which beam deformations extend into the wall, shown in Fig. 9 (from Wight and MacGregor, 2009) as  $h_b/2$  into each wall. This relationship has been suggested for cast-in-place systems; however, the simplified construction method proposed as part of this project, which takes advantage of precast coupling beams shallowly embedded into the cast-in-place walls, may behave differently. Thus, the proposed method may require a different equivalent beam length to approximate expected beam rotations.

For the coupled wall tested, Eq. 1 would predict beam rotations 2.1 times greater than the wall rotations. In this case,  $\ell$  is assumed to be the distance between the centroidal axes of the uncracked walls. Although the relationship between the beam and wall rotations varied throughout the test, results indicate that  $\theta_b \approx (1.5 - 2.0) \cdot \theta_w$ . It thus appears that the model used for cast-in-place systems may be slightly conservative, but reasonable for use in coupled wall systems with precast HPFRC coupling beams. Additional experimental data, however, are needed to fully validate this observation.

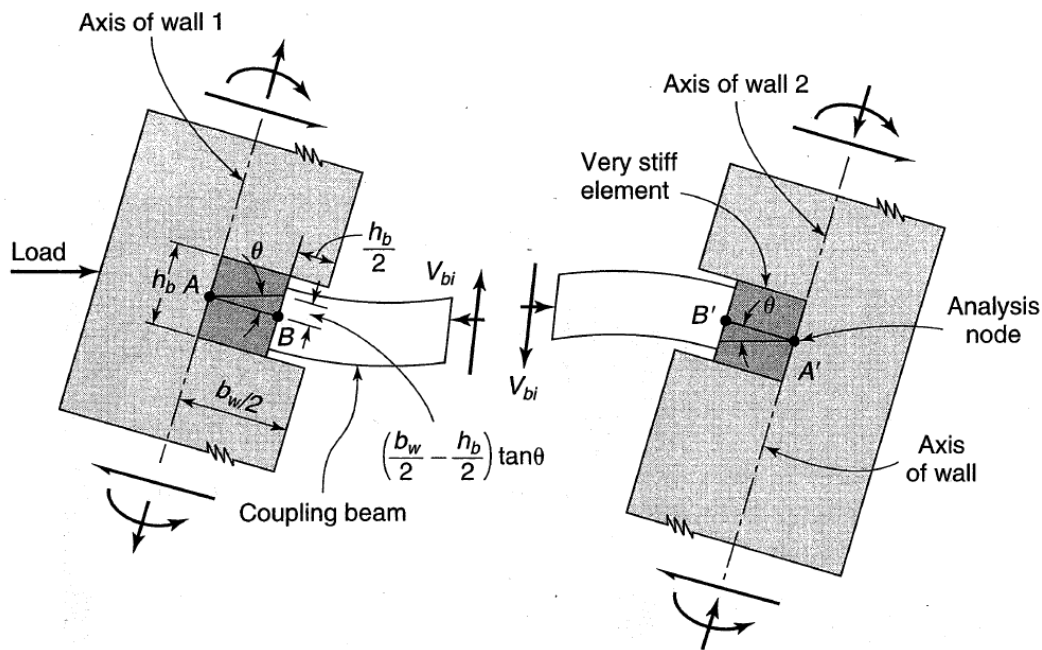


Fig. 9 - Coupling beam rotations (Wight and MacGregor, 2009)

## SUMMARY AND CONCLUSIONS

A large-scale four story coupled-wall specimen was constructed and tested to investigate the impact that precast HPFRC coupling beams have on the design, construction, and behavior of coupled-wall systems. Although at the time of this paper submission a second complementary coupled-wall specimen is in the process of being tested, the following preliminary conclusions can be drawn from the test described herein.

- Placing the precast coupling beams proved to be simple and is believed to be a viable alternative method for assembling a coupled-wall system. The proposed development detail allows for the structural wall reinforcement to continue, uninterrupted, through the connection with the coupling beam.
- For precast coupling beams, terminating even moderate amounts of longitudinal reinforcement within the wall near the interface is not recommended. This is believed to have caused a concentration of damage along the precast/cast-in-place interface at larger coupling beam drifts that was not observed in component tests with fully developed longitudinal reinforcement designed as described in Lequesne et al. (2009).

However, the overall system behavior was not significantly impacted by this localization of damage at the coupling beam/wall interface.

- The observed coupling beam rotations, relative to the structural wall drift, were slightly less than those predicted by existing design methods. The proposed precast connection scheme does not seem to significantly impact the relevance of the predictive models traditionally used for cast-in-place systems.
- It is recommended that for systems coupled by ductile HPFRC coupling beams, the expected ultimate capacities for the individual beams and walls should be used to define the design coupling ratio for the system. It was shown that the design coupling ratio, defined in this manner, is achieved at relatively moderate drift levels and largely maintained until failure of the system.
- Measurements taken throughout the test indicate that the tendency for coupling beams to elongate when subjected to reversing displacements is restrained by the adjacent structural walls and floor slabs. When correlated to component tests of coupling beams, the axial elongations permitted by the walls (shown in Fig. 8) imply the development of significant axial forces that will impact both the strength and ductility of the beams.
- The cast-in-place slab adjacent to the precast beam did not develop appreciable differential displacements relative to the beam until system drifts exceeded 1.5%. Even at these large drifts, the interface between the slab and beam was largely undamaged.
- Although not a focus of the current study, the ACI Building Code requirements for structural wall design provided adequate shear resistance and confinement of longitudinal reinforcement to allow for a stable flexural mechanism to develop in the base of both walls.

## ACKNOWLEDGEMENTS

This research project is funded by the National Science Foundation under Grant No. CMS 0530383. It is a part of the NEES research program. Special thanks go to Bekaert Corp. and Erico Corp. for donations of materials used in construction of the specimen described herein. The ideas and conclusions expressed are those of the writers, and do not necessarily represent the views of the sponsors.

## REFERENCES

- ACI Committee 318, 2008, *Building Code Requirements for Structural Concrete (ACI 318-08) and Commentary*, American Concrete Institute, Farmington Hills, MI, 465 pp.
- Aktan, A. E.; Bertero, V. V., 1984, "Seismic Response of R/C Frame-Wall Structures," *ASCE Journal of Structural Engineering*, V. 110, No. 8, pp. 1803-1821.
- ASCE/SEI 41/06, 2007, *Seismic Rehabilitation of Existing Buildings*, American Society of Civil Engineers, Reston, Virginia.
- ASTM C 1609/C 1609M – 05, 2005, "Standard Test Method for Flexural Performance of Fiber-Reinforced Concrete (Using Beam With Third-Point Loading)," West Conshohocken, PA.
- Canbolat, B. A.; Parra-Montesinos, G. J.; and Wight, J. K., 2005, "Experimental Study on Seismic Behavior of High-Performance Fiber-Reinforced Cement Composite Coupling Beams," *ACI Structural Journal*, V. 102, No. 1, pp. 159-166.
- Chao, S. H., 2005, *Bond Characterization of Reinforcing Bars and Prestressing Strands in High Performance Fiber Reinforced Cementitious Composites Under Monotonic and Cyclic Loading*, Ph.D. Dissertation, University of Michigan, Ann Arbor, MI, 475 pp.
- Gong, B.; and Shahrooz, B. M., 2001, "Concrete-Steel Composite Coupling Beams II: Subassembly Testing and Design Verification," *Journal of Structural Engineering*, V. 127, No. 6, pp. 632-638.
- Kwan, A. K. H.; and Zhao, Z. Z., 2002, "Cyclic Behaviour of Deep Reinforced Concrete Coupling Beams," *Structures and Buildings*, V. 152, No. 3, pp. 283-293.

- Lequesne, R.; Setkit, M.; Parra-Montesinos, G. J.; and Wight, J. K., 2009, "Seismic Detailing and Behavior of Coupling Beams with High-Performance Fiber Reinforced Concrete," *Antoine E. Naaman Symposium – Four decades of progress in prestressed concrete, fiber reinforced concrete, and thin laminate composites*, ACI Special Publication – *In Press*.
- Liao, W. C.; Chao, S. H.; Park, S. Y.; and Naaman, A. E., 2006, *Self-Consolidating High Performance Fiber Reinforced Concrete (SCHPFRC) – Preliminary Investigation*, Technical Report No. UMCEE 06-02, University of Michigan, Ann Arbor, MI, 68 pp.
- Paulay, T.; Taylor, R. G., 1981, "Slab Coupling of Earthquake-Resisting Shearwalls," *ACI Structural Journal*, V. 78, No. 2, pp. 130-140.
- Teshigawara, M.; Kato, M.; Sugaya, K.; Matsushima, Y., 1998a, "Energy Absorption Mechanism and the Fluctuation of Shear Force in the Coupled Shear Walls," *Structural Engineers World Congress 1998*, Paper Number T-186-5, Elsevier Science Ltd.
- Teshigawara, M.; Sugaya, K.; Kato, M.; Matsushima, Y., 1998b, "Seismic Test on 12-Story Coupled Shear Wall with Flange Walls," *Structural Engineers World Congress 1998*, Paper Number T-186-4, Elsevier Science Ltd.
- Wight, J. K.; and MacGregor, J. G., 2009, *Reinforced Concrete: Mechanics and Design*. 5<sup>th</sup> ed. p 943. Reprinted by permission of Pearson Education, Inc., Upper Saddle River, New Jersey.
- Zhao, Z. Z.; and Kwan, A. K. H., 2003. "Nonlinear Behavior of Deep Reinforced Concrete Coupling Beams." *Structural Engineering and Mechanics*, V. 15, No. 2, pp. 181-198.